

A new highly responsive material: spin fluctuations and superconductivity in FeNiB₂ system

Renhai Wang,^{1,2} Yang Sun,^{2,*} Vladimir Antropov,^{2,†} Zijing Lin,¹ Cai-Zhuang Wang,^{2,3} and Kai-Ming Ho^{2,3,4}

¹Department of Physics, University of Science and Technology of China, Hefei 230026, China

²Ames Laboratory, US DOE, Ames, Iowa 50011, USA

³Department of Physics, Iowa State University, Iowa 50011, USA

⁴International Center for Quantum Design of Functional Materials (ICQD),
Hefei National Laboratory for Physics Sciences at the Microscale,
University of Science and Technology of China, Hefei 230026, China

(Dated: Aug. 2, 2019)

By analyzing Fe-Ni-B compositional diagram we predict a new energetically and dynamically stable FeNiB₂ compound. This system belongs to the class of highly responsive state of material, as it is very sensitive to the external perturbations. This state is also characterized by a high level of spin fluctuations which strongly influence possible magnetic long- and short-range orders. Furthermore, we demonstrate that these antiferromagnetically dominating fluctuations could lead to the appearance of spin mediated superconductivity. The obtained results suggest a promising avenue for the search of strong spin fluctuation systems and related superconductors.

Introduction - Spin fluctuations (SF) in itinerant electron magnets play an important role in many metallic systems including weak itinerant magnets, heavy fermion compounds, actinides, Invar alloys and many magnetoresistive materials. SF also have been identified in high-temperature superconductors [1] and recently discovered Fe-based superconductors [2] with a clear suggestion about their crucial influence on the mechanisms of unconventional superconductivity. In the majority of cases superconductivity appears near magnetic quantum critical point, where magnetism has a pure itinerant character with no local moments involved. This is exactly a case when quantum SF (including spin zero-point motion) are strong and provide a dominating contribution to many observable physical properties. However, as a typical example, in a case of superconductivity, the direct calculations and prediction of critical temperature from first principle is still not possible. In this situation one can focus on searching for new materials with a strong level of SF, leading to possible development of promising physical properties.

Here we will introduce qualitatively the concept of a highly responsive state (HRS) (see Fig. 1). This term is used here to indicate that a physical system is in a state characterized by an order parameter which is very sensitive to the external perturbations (temperature, pressure, magnetic fields, etc.). The HRS state is naturally related with a closeness to the instability and, as usual in such situations, one can expect that fluctuations are very important.

To search for new material of such type we start our study with a less known system Fe-Ni-B in the concentration regime where magnetism is not supposed to be very strong (equal concentration of magnetic 3d atoms and nonmagnetic B atoms). Further we proceed with a structural search for new stable compounds and then study the stability of predicted antiferromagnetic (AFM)

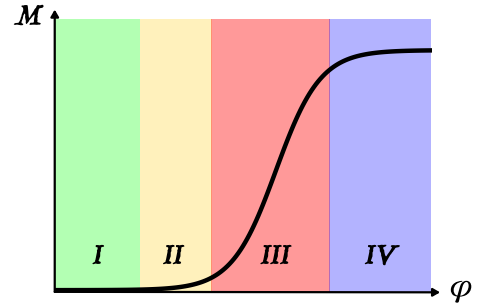


FIG. 1. Schematics of HRS from a viewpoint of mean field description. Regions I and IV represent nonmagnetic and saturated regimes; Region II corresponds to quantum critical point and a system in the area III is in HRS regime with possible large gradients of magnetization and strong spin fluctuations. M is the order parameter while φ is the external perturbation (pressure, temperature, magnetic field, etc).

order by adding possible SF in the ground state (quantum zero-point motion). At the end we estimate the influence of quantum SF on possible appearance of SF induced superconductivity.

Structure prediction - Crystal structures of Fe-Ni-B were searched by an adaptive genetic algorithm (AGA), which integrates auxiliary interatomic potentials and first-principles calculations together in an adaptive manner to ensure the high efficiency and accuracy (see Supplementary Materials for more details) [3, 4]. The structure searches were only constrained by the chemical composition, without any assumption on the Bravais lattice type, symmetry, atom basis or unit cell dimensions. A range of different composition around the FeNiB (111) compositional ratio (i.e., 211, 121, 112, 311, 131, 113, 221, 122, 212, 133, 313, 331, 321, 312, 123, 132, 231, 213, 223, 232, 322, 233, 323 and 332) were selected with 2 and 4 formula units to perform the AGA search. First-

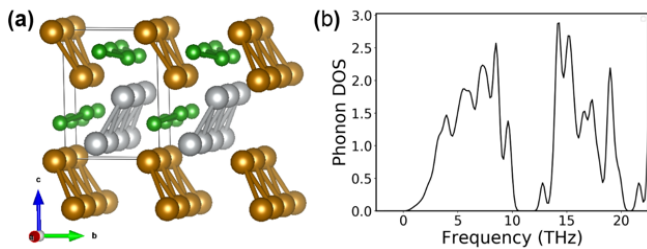


FIG. 2. (a) The configuration of FeNiB_2 from AGA search. Atom color: Fe atoms colored with brown; Ni atoms colored with silver; B atoms colored with green. (b) Phonon density of States.

principles calculations were carried out using the projector augmented wave (PAW) method [5] within density functional theory (DFT) as implemented in VASP code [6, 7]. The exchange and correlation energy is treated within the spin-polarized generalized gradient approximation (GGA) and parameterized by Perdew-Burke-Ernzerhof formula (PBE) [8]. A plane-wave basis was used with a kinetic energy cutoff of 520 eV. During the AGA search, Monkhorst-Pack’s sampling scheme [9] was adopted for Brillouin zone sampling with a k-point grid of $2\pi \times 0.033 \text{ \AA}^{-1}$, and the ionic relaxations stopped when the forces on every atom became smaller than 0.01 eV/Å. The energy convergence criterion is 10^{-4} eV. The phonon calculations were performed with the finite difference method via Phonopy code [10]. The magnetic properties were calculated in a higher-quality calculation using a finer k-point sampling grid of spacing $2\pi \times 0.02 \text{ \AA}^{-1}$ and a stricter energy convergence criterion of 10^{-6} eV.

Among all AGA searched ternary phases, a new FeNiB_2 phase, with 2 formula units and a space group of $P2_1/m$ (space group number 11), is found to show the energy even smaller than the Gibbs triangle formed by the existing stable phases on the ternary phase diagram. The structure of this new phase is shown in Fig. 2(a). There is one Wyckoff site for Fe, Ni and two Wyckoff sites for B, respectively (the crystallographic details are given in Supplementary Materials). The Fe, Ni and B atoms formed separated 1D chain. Phonon calculation further confirmed the phase is dynamically stable without any soft phonon mode at $T = 0$ K, which is shown in Fig. 2(b).

With the newly found FeNiB_2 structure, the existing Fe-Ni-B phase diagram should be updated. In the current DFT-calculated database (i.e., the Materials Project [11]), there are eight reported binary stable phases however there is no ternary stable phase reported. It should be noted that while the experimental database (i.e. Inorganic Crystal Structure Database [12]) shows that a few ternary phases such as FeNiB , Fe_2NiB , $\text{Fe}_3\text{Ni}_3\text{B}_2$ and $\text{Fe}_3\text{Ni}_{20}\text{B}_6$ previously synthesized by experiments, they

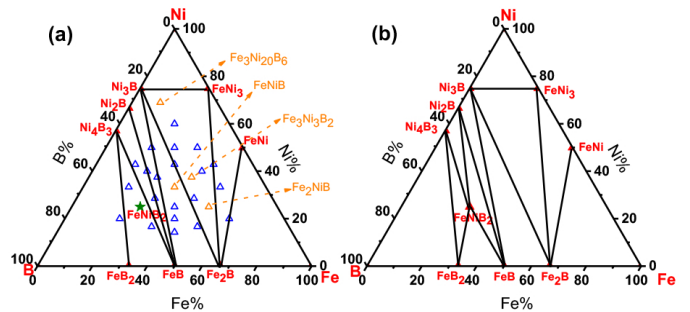


FIG. 3. DFT-calculated convex hull of the Fe-Ni-B system based on (a) previously reported phases and (b) after including the newly discovered FeNiB_2 phase. All DFT calculations were carried out at 0 K. Red solid triangles represent stable compounds and the green solid star represent newly found stable phase, while blue and orange open triangles indicate the metastable phases from AGA search and experiments, respectively. The black lines separate the compositional space to Gibbs triangles.

are all metastable phases according to DFT calculations, indicating they may decompose to the surrounding stable phases on the Gibbs triangle in the equilibrium state [13, 14]. The existing ternary convex hull computed from DFT calculation are shown in Fig. 3(a) (the detailed energy values are provided in Supplementary Materials). At the composition of FeNiB_2 , the thermodynamic stability is determined by the Gibbs triangle formed by the nearby Ni_4B_3 , FeB , and FeB_2 phases. Considering the following reaction $\text{FeNiB}_2 \rightarrow (\text{Ni}_4\text{B}_3 + 3\text{FeB} + \text{FeB}_2)/4$, FeNiB_2 is a stable phase if the formation energy of the left hand side is lower than that of the right hand side. The DFT calculations indeed show that the formation energy of FeNiB_2 in the $P2_1/m$ structure is equal to -340.9 meV/atom, while at the right-hand side, i.e. the energy on the convex hull at the composition of FeNiB_2 , is calculated to be -326.57 meV/atom. Therefore, FeNiB_2 is thermodynamically stable at the temperature of 0 K and the convex hull of the Fe-Ni-B system should be updated with the inclusion of the new FeNiB_2 phase. The new phase diagram of Fe-Ni-B system at 0 K are show in Fig. 3(b).

With the verified stability of the new FeNiB_2 structure we are now in position to investigate its magnetic ground state. The DFT calculations are performed for the ferromagnetic (FM) state and the simplest AFM state, in which two Fe atoms in the primitive cell show opposite spin directions. It shows a strong competition of energetic stability between the FM and AFM states in the FeNiB_2 structure at 0 K. As shown in Fig. 4(a), the two states exhibit very similar energies, while the AFM state has a slightly lower energy ~ 0.45 meV/atom at the equilibrium volume $7.8 \text{ \AA}^3/\text{atom}$. As the volume increases, the energy difference becomes larger and the AFM state is always slightly more stable than FM state. More in-

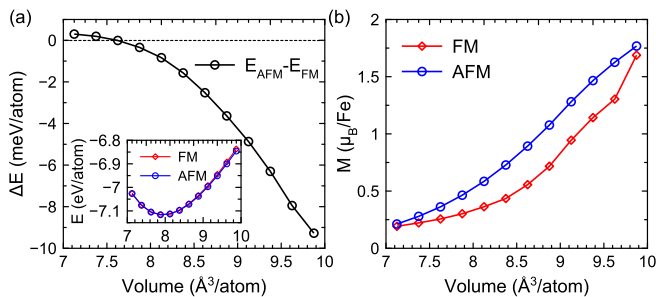


FIG. 4. (a) The energy difference and (b) the Fe magnetic moment at AFM and FM states as a function of the volume for the FeNiB₂ structure. The insert in (a) shows the total energies for both configurations.

Interestingly, in Fig. 4(b), the equilibrium magnetic moments demonstrate a rapid increase (nearly by 10 times) while Neel temperature also becomes nearly 50 – 60 K (mean field estimate). It suggests the FeNiB₂ structure is locating in the highly responsive state (region III in Fig. 1). Coexistence of different magnetic long-range orders even for small values of atomic magnetic moments indicates that energy profile should have many local minima without well-defined global minimum. Correspondingly, the system is very sensitive to any external perturbation and could easily change its magnetic state (“magnetic chameleon”).

The effects of zero-point spin fluctuations on the magnetic stability of the ground state of FeNiB₂ - Let us first address the issue of magnetic instability in FeNiB₂. Our nonmagnetic calculations of this system revealed that the density of states (DOS) at the Fermi level is dominated by Fe electrons. So the Stoner criterion is fulfilled

$$1 - I\chi_0 > 0. \quad (1)$$

Here χ_0 is non-enhanced magnetic susceptibility, while I is the effective Stoner parameter of static LDA. For mul-

ticomponent system the corresponding Stoner criterion was obtained in Ref. [15] and is written as

$$N_t(E_F) I > 1 \text{ or } \sum_i I_i N_i^2 > N_t, \quad (2)$$

where the effective Stoner parameter I for multicomponent system is defined as $I = \sum_i I_i \left(\frac{N_i}{N_t}\right)^2$, where I_i and N_i are partial Stoner parameter and partial DOS at the Fermi level, correspondingly, and N_t is the total DOS at the Fermi level. The obtained numbers are shown in Table I and the resulting criteria of possible long-range AFM order is fulfilled. Such criteria are also fulfilled at many other q -vectors, including FM one. We also found that criteria of a local magnetic moment stability (Anderson criteria) is satisfied as well.

However, LDA traditionally overestimates the magnetism for weakly magnetic systems due to neglect of

TABLE I. The partial density of state at the Fermi level and the Stoner parameter at each atom for FeNiB₂.

	DOS @ E_f (State/eV)	I (eV)
Total (N_t)	1.962	
Fe	1.477	0.84
Ni	0.312	0.87
B	0.0895	2.20

quantum SF at $T = 0$ K (spin zero-point motion). To study the stability of predicted above weak magnetism in FeNiB₂ we used a modified version of SF theory from Ref.[16]. First, we obtain the *ab initio* SF energy (absent in LDA) using RPA technique [17]. Then we calculate a corresponding SF contribution to the spin susceptibility and finally obtain renormalized Stoner criterion for magnetic instability.

The following RPA expression for the SF contribution to the total energy has been used

$$E_{SF} = \lim_{T \rightarrow 0} F_{SF} = 2\hbar \lim_{T \rightarrow 0} \sum_v \int_0^I dI \int_{\Omega_{BZ}} d\mathbf{q} \int_{-\infty}^{\infty} d\omega (\text{Im}\chi_v(\mathbf{q}, \omega) - \text{Im}\chi_{v0}(\mathbf{q}, \omega)) \coth(\beta\omega/2). \quad (3)$$

This expression can also be rewritten as

$$E_{SF} = \frac{1}{2} \int_0^I dI (\langle M^2 \rangle - \langle M_0^2 \rangle), \quad (4)$$

where $\langle M^2 \rangle$ is a square mean of magnetic moment obtained with enhanced and nonenhanced susceptibility, correspondingly (see Fig.8 in Ref.[18] for detailed definition and calculations of these quantities in pure 3d metals). Computational details of our linear response method can be found in Ref.[18].

The transverse part of SF correction to the inverse magnetic susceptibility is obtained directly as

$$\chi_{SF}^{-1} = \frac{1}{2M} \frac{\partial}{\partial M} \left(\int_0^I dI (\langle M^2 \rangle - \langle M_0^2 \rangle) \right). \quad (5)$$

This expression is different from the one used in Refs.[16, 19] as we do not employ low frequency and long wavelength approximations [20]. The SF renormalized

Stoner criterion then is written as

$$(\chi_{SF}^{-1} + \chi^{-1}) \chi_0 = 1 - I^* \chi_0 > 0, \quad (6)$$

where I^* is a renormalized Stoner parameter, which includes quantum spin zero points SF beyond usual static local density approximation. This renormalization was first noticed by Moriya [16] and studied recently using electronic structure calculations in Ref. [19] for several simple 3d metals. All these studies have been performed using *ad-hoc* low frequency and long wave approximations. Our approach is truly ab-initio and takes into account SF at all q vectors and frequencies.

Our results indicated that the SF renormalization of the effective Stoner parameter in FeNiB₂ is nearly 7% with dominating suppression coming from Fe sites. Many different SF with q -vectors around AFM instability contribute to this suppression in the frequency range up to 0.3 eV, but overall transitions inside electronic d-band (4–5 eV) contribute to this renormalization. It suggests that the existence of predicted SF can be measured by neutron scattering experiments. Both longitudinal and transversal SF on Ni sites are also strong but due to small original static moment on Ni atoms, the Ni contribution

to the total magnetization suppression is small.

The appearance of AFM like magnetic instability can also be favorable for SF induced superconductivity. While s-wave and triplet superconductivity could theoretically appear near FM instability, such systems are not really known. Superconductivity reports in weakly FM system ZnZr₂ under pressure have not been confirmed. But more popular singlet superconductivity can naturally appear near AFM instability (cuprates [1], iron pnictides [2]). So, the appearance of superconductivity looks possible in this system and now we will estimate a strength of electron-spin interaction and its contribution to SF induced superconductivity.

The effects of zero-point spin fluctuations on superconductivity in FeNiB₂ - From practical point of view, e.g., for the search of new superconducting material, the qualitative estimation of λ is of primary interest. To obtain the required strength of spin-electron interaction we will use well known s-d exchange model [21]. To estimate λ we do not need to consider the superconducting phase since it enters just the mass renormalization in the normal state and one needs just to deal with the corresponding expression for the electron self-energy [19],

$$\Sigma_{\mathbf{k}}(E) = I^2 \sum_{\mathbf{q}} \int_0^{\infty} \frac{d\omega}{4\pi} \text{Im}\chi(\mathbf{k} - \mathbf{q}, \omega) \left[\frac{1 - f_{\mathbf{q}}}{E - \varepsilon_{\mathbf{q}} - \omega} + \frac{f_{\mathbf{q}}}{E - \varepsilon_{\mathbf{q}} + \omega} \right], \quad (7)$$

where $f_{\mathbf{q}}$ is the Fermi distribution with $\varepsilon_{\mathbf{q}}$ being one electron spectrum. The expression for the coupling constant at $T = 0$ K is then written in standard way as

$$\lambda = - \left. \frac{\partial \langle \Sigma_{\mathbf{k}}(E) \rangle}{\partial E} \right|_{E=0}. \quad (8)$$

To make the simplest possible estimation of electron magnon interaction one can replace the average over the Fermi surface above by the average over the Brillouin zone. To further obtain the temperature of the superconducting transition using the approach advocated above we use usual MacMillan formula [22]. Under these approximations our calculated value of $\lambda = 0.6$ and the effective SF frequency is $\omega = 0.2$ eV. With these numbers we obtain a value of 20 – 30 K for the critical temperature. Thus, our qualitative estimation predicts not only suppression of magnetic long-range order in the normal state but also suggest a very promising scenario for the SF induced superconductivity near AFM quantum critical point.

In summary, we performed a structural search for a new stable system near magnetic instability. Our AGA approach which integrates auxiliary interatomic poten-

tials and first-principles calculations found a new stable compound FeNiB₂, which appears to be a magnetically highly responsive system close to antiferromagnetic instability. This system is characterized by strong SF at $T = 0$ K (quantum spin zero-point motion) and possible SF induced superconductivity. The experimental verifications of our prediction are highly desirable. Our magneto-structural combined studies thus open a new route for the search of strong SF state and superconductors.

Acknowledgements Work at Ames Laboratory was supported by the U.S. Department of Energy, Basic Energy Sciences, Materials Science and Engineering Division, under Contract No. DEAC02-07CH11358, including a grant of computer time at the National Energy Research Scientific Computing Center (NERSC) in Berkeley, CA. Work at University of Science and Technology of China was supported by the National Natural Science Foundation of China (11574284 & 11774324) and the Supercomputing Center of the University of Science and Technology of China.

* Email: yangsun@ameslab.gov

† Email: antropov@ameslab.gov

- [1] T. Moriya and K. Ueda, *Adv. Phys.* 49, 555 (2000).
- [2] D. C. Johnston, *Adv. Phys.* 59, 803 (2010).
- [3] S. Q. Wu, M. Ji, C. Z. Wang, M. C. Nguyen, X. Zhao, K. Umemoto, R. M. Wentzcovitch, and K. M. Ho, *J. Phys. Condens. Matter* 26, 035402 (2014).
- [4] X. Zhao, M. C. Nguyen, W. Y. Zhang, C. Z. Wang, M. J. Kramer, D. J. Sellmyer, X. Z. Li, F. Zhang, L. Q. Ke, V. P. Antropov, and K. M. Ho, *Phys. Rev. Lett.* 112, 045502 (2014).
- [5] P. E. Blchl, *Phys. Rev. B* 50, 17953 (1994).
- [6] G. Kresse and J. Furthmller, *Comput. Mater. Sci.* 6, 15 (1996).
- [7] G. Kresse and J. Furthmller, *Phys. Rev. B* 54, 11169 (1996).
- [8] J. P. Perdew, K. Burke, and M. Ernzerhof, *Phys. Rev. Lett.* 77, 3865 (1996).
- [9] H. J. Monkhorst and J. D. Pack, *Phys. Rev. B* 13, 5188 (1976).
- [10] A. Togo and I. Tanaka, *Scr. Mater.* 108, 1 (2015).
- [11] A. Jain, S. P. Ong, G. Hautier, W. Chen, W. D. Richards, S. Dacek, S. Cholia, D. Gunter, D. Skinner, G. Ceder, and K. A. Persson, *APL Mater.* 1, 011002 (2013).
- [12] M. Hellenbrandt, *Crystallogr. Rev.* 10, 17 (2004).
- [13] Y. Khan, *Z. Met.* 74, 385 (1983).
- [14] C. Gianoglio and C. Badini, *J. Mater. Sci.* 21, 4331 (1986).
- [15] T. Jarlborg and A. J. Freeman, *Phys. Rev. B* 22, 2332 (1980).
- [16] T. Moriya and A. Kawabata, *J. Phys. Soc. Japan* 34, 639 (1973).
- [17] F. Englert and R. Brout, *Phys. Rev.* 120, 1085 (1960).
- [18] A. L. Wysocki, V. N. Valmispild, A. Kutepov, S. Sharma, J. K. Dewhurst, E. K. U. Gross, A. I. Lichtenstein, and V. P. Antropov, *Phys. Rev. B* 96, 184418 (2017).
- [19] V. P. Antropov and A. Solontsov, *J. Appl. Phys.* 109, 07E116 (2011).
- [20] V. P. Antropov, *J. Magn. Magn. Mater.* 262, L192 (2003).
- [21] V. Y. Irkhin and M. I. Katsnelson, *Z. Phys. B* 75, 67 (1989).
- [22] W. L. McMillan, *Phys. Rev.* 167, 331 (1968).